Indian J Phys (December 2024) 98(14):4919–4932
https://doi.org/10.1007/s12648-024-03214-3

ORIGINAL PAPER

Optimization of hydrophobic anti-reflection calcium fluoride films for ZnO/GaAs heterojunction solar cell: a simulation study

S Maqsood[1,2,4], M Ishaq[3,4], Z Ali[1,4], K Ali[1,4]* and B Hussain[3,4]

[1]Nano-Optoelectronics Research Laboratory, Department of Physics, University of Agriculture Faisalabad, Faisalabad 38040, Pakistan

[2]Department of Physics, Government College Women University Faisalabad, Faisalabad, Pakistan

[3]Riphah International University Faisalabad, Faisalabad, Pakistan

[4]Intel Corporation Rio Rancho, Rio Rancho, NM 87124, USA

Received: 28 August 2023 / Accepted: 16 April 2024 / Published online: 14 May 2024

Abstract: In this work, calcium fluoride (CaF_2) has been employed as an anti-reflection coating (ARC) for gallium arsenide (GaAs) based heterojunction solar cell. A numerical analysis was carried out to optimize performance parameters such as doping concentration, thickness of absorber and window layer, and carrier lifetime. ZnO and GaAs have been employed as window and absorber layer, respectively. Performance of CaF_2 ARC has been investigated at optimum conditions. Personal computer one-dimensional simulator has been used for numerical analysis. Different Materials like magnesium oxide, magnesium fluoride (MgF_2), titanium nitrate, aluminum trioxide and silicon dioxide, have been considered to make a comparative analysis. Best power conversion efficiency of 27.4% has been achieved with 32.0 mA short circuit current, 0.9899 V of open circuit voltage, and 86.49% of fill factor at optimum thicknesses of ARC, absorber, and window layers. Results revealed that MgF_2 and CaF_2 show almost same results as ARC layer but when it comes to stability CaF_2 is more appropriate material as ARC layer for ZnO/GaAS solar cell. The results prove that optimization of thickness of materials, doping concentration, and carrier lifetime of absorber and window layer would make the crucial factor to fabricate the cost efficient and highly efficient GaAs solar cell based on CaF_2 ARC layer.

Keywords: ZnO; GaAs solar cells; Power conversion efficiency; PC1D; Antireflection layer; Optoelectrical properties

1. Introduction

The continuous growth in global population with current rate will lead to 100% increase in world's electricity consumption by 2050 [1]. Fossil fuel energy utilization is causing alarming rise in the CO_2 emission drawing the attention of researchers more towards the renewable sources of energy [2, 3]. Solar energy is a well-known clean energy resource therefore, relevant research community is concentrating on developing solar energy technology and trying to make it competitive with conventional energy resources [4, 5]. Among all, silicon based cells are extensively used in photovoltaic (PV) industry [6, 7]. However, c-Si based solar cells have indirect band gap and require active layers thick enough (greater than 200 μm) to capture incoming sunlight increasing the cost of PV devices [8, 9].

III-V semiconductor materials are used in second generation solar cells due to their direct bandgap that allows significantly thinner absorbing layer. Among III-V semiconductors, Copper Indium Gallium Selenide (CIGS), Gallium Arsenide (GaAs), and Cadmium Telluride (CdTe) are the promising materials to improve the performance of solar cells. Though, Se and Cd are toxic, while Te and In are rare elements, these constraints are the major obstacles in the production of low-cost CIGS and CdTe solar cells. The ideal solar cell should be less expensive and work more efficiently, which are conflicting goals. Thin film solar cells can potentially achieve these goals because of significantly lower material cost [10]. GaAs is a well-known semiconductor material used in high-efficiency thin film solar cells [11, 12]. GaAs thin films can be prepared by atomic beam sputtering [13], RF magnetron sputtering [14], and chemical deposition [15]. GaAs is a more

*Corresponding author, E-mail: khuram_uaf@yahoo.com

suitable solar energy material due to its absorption coefficient similar to silicon with 1.42 eV bandgap energy [16, 17] and high electron mobility (9000 cm^2/V.s at 300 K) [18, 19]. For GaAs based solar cells, the Hanergy Group reported a 29.1% record breaking efficiency being tested on NASA international space station [20]. Kuang, et al. reported PCE from 0.772 to 2.218% by varying thicknesses and doping concentration of GaAs layer using TCAD software in graphene/GaAs/SiO_2/Au junction solar cell [21]. Mohamed, et al. used AMPS-1D simulator to analyze the GaAs solar cell efficiency that are fabricated with double junction cell combined with Galium Indium Phosphide (GaInP). From simulation it can be seen that increase in thickness of GaAs layer and decreases in thickness of GaInP enhances the efficiency [22]. Degradation and radiation losses of the GaAs absorber layer is a major concern in solar cells [23, 24]. This effect can be reduced by using a window layer with appropriate bandgap and robustness [3]. To choose a suitable window layer some important properties must be considered like high transmittance and electrical conductivity [25].

ZnO is an emerging material in semiconductor industry. Due to its simple processing steps, low deposition temperature, abundance, low fabrication cost, low toxicity, stable wurtzite structure, and 1.603 is lattice c/a ratio which is near to the ideal ratio of 1.633, it is a promising material in heterojunction solar cells as a window layer [26–30]. Additionally, ZnO is more radiation resistant than GaN, Si and GaAs which reduces photo-degradation and provides prolong device lifetime. Apart from a variety of additional features that distinguish ZnO as a unique wide bandgap material, its electron affinity and bandgap can be modified over a wide range by alloying or doping. In order to generate high photocurrent, the solar cell should absorb maximum photons from the incident source of light [31–33]. One of the major sources of optical loss is reflection. To reduce reflection losses, ARC layers are frequently used for light trapping [34, 35]. Many researchers utilized different materials for ARC layer to enhance the solar cell efficiency such as titanium dioxide (TiO_2) [36, 37], aluminum trioxide (Al_2O_3) [38], magnesium fluoride (MgF_2) [39], silicon carbide (SiC) [40], magnesium oxide (MgO) [41], strontium fluoride (SrF_2) [42], titanium nitride (TiN) [43], zinc selenide (ZnSe) [44–46] and zinc sulfide (ZnS) [47, 48]. MgF2/ZnS, with refractive indices of 1.38 and 2.32 respectively, is most commonly used ARC in AlGaAs/GaAs solar cells and can pass radiations in the 400–1400 nm range. Stable and long-lasting coatings can be produced by using materials like ZrO_2, HfO_2 and TiO_2 as a bottom layer and SiO_2 or Al_2O_3 as an upper layer [49]. Fedawy, M. et al. used Si_3N_4 ARC layer on GaAs single junction solar cell and reported 27.16% efficiency at optimum thickness of 75 nm [50]. KC, D et al. reported 31.1% efficiency with window layer of AlGaAs at base layer thickness of 2.2 μm with doping concentration of 1×10^{16} cm^{-3} and temperature of 25 °C by using PC1D simulation [16]. Kuamar, et al. reported 16.64% average reflectance without any ARC layer for GaAs solar cell and average reflectance (R_{av}) was observed to be reduced up to 4.85% in the range of wavelength 400–1200 nm by applying ARC layer of Al_2O_3 [3]. Despite the fact, majority of these materials have excellent performance, scale-up and the integration of the majority of these processes are complex or expensive.

In this paper we propose CaF_2 as an AR coating for ZnO/GaAs heterojunction solar cell. PC1D simulator is used to optimize the parameters like thickness, doping concentration, and carrier lifetime of window and absorber layer at 25 °C temperature. The study showed that the highest PCE of 27.4% with Isc of 32 mA, Voc of 0.9899, and FF Of 86.49% were attained by ZnO/GaAs solar cell with CaF_2 AR coating at optimum ARC thickness. While without any application of AR coating 24.5% PCE has been observed with 28.9 mA Isc, 0.9872 Voc and 85.87 FF.

This manuscript is assembled as follows: In Sect. 2, we establish the characteristics of different hydrophobic antireflection coatings. In Sect. 3, the model of proposed solar cell and values of parameters applied in simulation have been represented. In Sect. 4, we plot the performance parameter of proposed structure of cell such as Voc, efficiency and reflectance. Section 5 includes summary and conclusion.

2. Hydrophobic anti-reflection films

Hydrophobic anti-reflection films with high mechanical, thermal and chemical stability can play a significant role in windshields of automobiles, outdoor screen devices, solar panels and as well as other optical and optoelectronic elements. Such films prevent them from inevitable environmental circumstances like rain, wind, humidity, and dust while also assisting in maintaining good light transmittance [51–58]. The performance of optical devices like screen devices, automobile windshields and solar panels is badly affected by development of dust particles and moisture on surfaces that restrict the light transmission [51–55]. Quan et al. described the characterization and growth of hydrophobic SiO_2 layers that have self-cleaning properties and low dust particle adhesion [51, 59]. Solar cells and other devices should have transparent and protected front layer with low refractive index, wide band gap, broad wavelength range, high thermal and chemical stability, and low optical loss [58–60]. These requirements are accomplished by alkaline earth metal fluorides (MgF_2 and

CaF_2), which are already employed in optical devices and components like lenses, polarizers, and optical windows [61–66]. CaF_2 and MgF_2 are the promising candidates for optical devices due to their low refractive index. MgF_2 is widely used as AR material due to its outstanding optical properties [64, 66]. Calcium fluoride (CaF_2) films are another promising candidate for AR layers because of their low refractive index and their broad range of transmission wavelength [67–69]. CaF_2 films can be produced in crystalline structure without deliberately heating the substrate [70]. It features a conventional fluorite-cubic form, indicating that face-centered cube having four Ca_2 + associating each F^- and eight F^- associating each Ca^{2+} [67, 68]. MgF_2 is often deposited at room temperature by thermal evaporation [71], which results in amorphous, metastable films [72, 73]. In contrast, c-CaF_2 thin films are thermally stable and are therefore appropriate for the fabrication of devices. CaF_2 has high relative permittivity of 8.4, low refractive index in infrared (IR) region (n = 1.42 for λ = 1 μm), it also has a broad transmittance spectrum from 130 to 10,000 nm, relatively high dielectric constant ($\sim$ 6.8) and wide band gap of 12 eV [61, 67].

To determine the crystal structure of the deposited CaF_2 thin films, XRD is utilized. An Ambios Q-scope atomic force microscope and FESEM is used to visualize the film's surface shape. The AFM can be used to calculate the roughness's root mean square (RMS). A Filmetrics F20 instrument can measure thickness, reflection, and refractive index. A UV/vis Lambda 2S spectrophotometer made by Perkin-Elmer can be used to determine the transmittance spectrum [74–76]. CaF_2 have higher dialectic constant as compared to commonly used ARC materials (SiO_2 and MgF_2). MgF_2 and CaF_2 showed the identical optical properties. Solubility expose that CaF_2 (16 mg L^{-1}) is less soluble in water than MgF_2 (76 mg L^{-1}). Chemical resistance of ARC layer against outdoor conditions like moisture and rain could be interesting factor. CaF_2 could be proven more weather-proof as compared to MgF_2 [76]. Unit cell characteristics of CaF_2 crystals are more closely match to various semiconductor materials making it suitable material in opto-electronic devices [77, 78]. Huang et al. suggested in their simulation study of heterostructure that the application of CaF_2 with the conjunction of Ge for cooling of optoelectronic devices meant to release heat in IR region (5–8 μm) [79]. Numerous chemical and physical techniques have been used to synthesize CaF_2 films such as electron beam evaporation, molecular beam epitaxy. magnetron sputtering, pulsed laser deposition, thermal evaporation, and electrodepositing [61–63, 67, 68, 77, 80]. Thin film form of CaF_2 is scarcely investigated and there are just a few reports on it in the literature [62, 67, 77, 81]. Daimonet et al. measured the refractive index of calcium fluoride with respect to wavelength by goniometer–spectrometer model 1 UVVIS-IR that was made by Moller-Wedel as shown in Fig. 1 [82].

3. Simulation parameters and device structure

In our proposed structure GaAs has been used as absorber layer and ZnO as window layer with an ARC film as demonstrated in Fig. 1. Coatings are arranged in order of decreasing band gap, material with the highest band gap on upper level and material that have lower band gap should be on bottom level [31, 83]. A material with a highest band gap can absorb energy at lower wavelengths [84, 85]. For the ARC layer, the refractive index is an essential metric. Reflection of light will be reduced from surface if refractive index of layer is geometrical mean of the two adjacent indices. ZnO has 2 refractive index and air has 1 at 600 nm [86]. The refractive index of ARC layer should be in between to 1(air) and 2 (ZnO) for this proposed heterojunction. If we consider proposed model, then ZnO is one side and air on the other so optimum refractive index is calculated by $n_1=\sqrt{n_0 n_2}$. The optimum value of refractive index for proposed model is 1.414 at wavelength that have peak intensity in region of solar spectrum. The refractive index of CaF_2 at 600 nm is 1.434 [82] which is near to the optimum value of refractive index for this model. The effects of changing electrical and physical properties on device performance can be understood through accurate simulation software. Several simulation software such as PC1D, AFORS-HET, Silvaco TCAD and Sentaurus TCAD, is available for solar cells [83, 87, 88]. PC1D, an open-source substitute, is also capable of simulating popular solar cells made of silicon and germanium. Several parameters can be adjusted to understand their impact on the device's overall performance, including doping levels, temperature, parasitic resistance, recombination, carrier lifetime, back surface fields and others. Results in graphical format can be obtained from PC1D, including short circuit

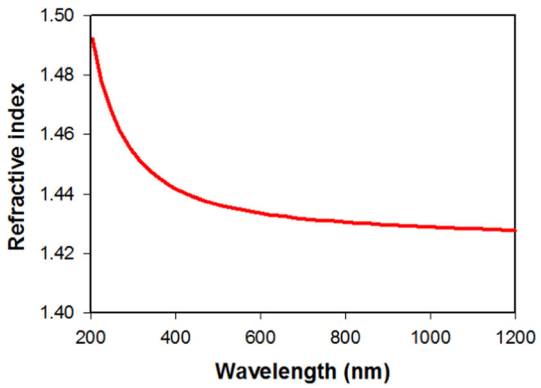

Fig. 1 Spectral behavior of n for CaF_2 [82]

Table 1 Parameters for optimum stimulated device

Parameters	GaAS	ZnO
Thickness	10–80 μm	0.5–4 μm
Band gap	1.42	3.27 eV
Electron affinity	4.07	4.5
Dielectric constant	13.18	8.66
Doping concentration	1×10^{12}–1×10^{18} cm^{-3}	1×10^{12}–1×10^{18} cm^{-3}
Electron mobility	–	50 cm^2/Vs
Hole mobility	–	50 cm^2/Vs
Other parameters	Internal PC1D	Internal PC1D

current (Jsc), current voltage (I-V) curves, open circuit voltage (Voc), etc. [89].

The following numerical equations are used in the PC1D simulation to simulate solar cells. Expressions (1)–(9) show how to build a model and altered process parameters [90].

$$j_n = \mu_n.n.\nabla E_{Fn} \tag{1}$$

$$j_p = \mu_p.p.\nabla E_{Fp} \tag{2}$$

The current densities of electrons and holes are represented as j_n and j_p, as presented in Eqs. (1) and (2), while μ_n *and* μ_p are electron and hole mobility.

$$\frac{\partial n}{\partial t} = \frac{\nabla . j_n}{q} + G_L - U_n \tag{3}$$

$$\frac{\partial p}{\partial t} = \frac{\nabla . j_p}{q} + G_L - U_p \tag{4}$$

$$\Delta^2 \varphi = \frac{q}{\varepsilon}(n - p + N^-{}_{acc} - N^+{}_{don}) \tag{5}$$

where U_n and G_L denotes the recombination and generation rate, $N^+{}_{don}$ and $N^-{}_{acc}$ denotes the donor and acceptor doping concentrations.

$$n = N_c F_{1/2}\left(\frac{q\psi + V_n - q\phi_{n,i} + \ln\left(n_{i,0}/N_c\right)}{K_B T}\right. \tag{6}$$

$$p = N_v F_{1/2}\left(\frac{-q\psi + V_p - q\phi_{p,i} + \ln\left(n_{i,0}/N_v\right)}{K_B T}\right. \tag{7}$$

N_c and N_v are the effective densities of states in the conduction and valence bands, respectively. Finally, the solar cell efficiency is calculated by given formula.

$$\eta = \frac{P_{max}}{P_{in}} = \frac{V_{oc} I_{sc} FF}{P_{in}} \tag{8}$$

where,$I_{sc}V_{oc}$ η, P_{in}, FF,I_{sc},V_{oc}, and P_{max} represents the short circuit current, efficiency, fill factor, input power, and maximum power.

In this work, the effect of hydrophobic CaF_2 thin films as ARC material for ZnO/GaAs heterojunction is analyzed using PC1D tool. Different materials were also used for comparative analysis with CaF_2 films. PC1D software is extensively used due to high calculation speed and easy interfacing. To determine the accurate reflectance, the parameters r, r_2, and θ are further estimated by the equations. The Mathematical Model satisfies the reflectance has been given below [34, 35]:

$$r_1 = \frac{\eta_0 - \eta_1}{\eta_0 - \eta_1} \tag{9}$$

$$r_1 = \frac{\eta_0 - \eta_1}{\eta_1 + \eta_2} \tag{10}$$

$$\theta = \frac{2\pi\eta_1 d}{\lambda} \tag{11}$$

For a single ARC layer, the reflectance can be extracted as equation

$$R = \left|r^2\right| = \frac{r_1^2 + r_2^2 + 2r_1 r_2 \cos 2\theta}{1 + r_1^2 + r_2^2 + 2r_1 r_2 \cos 2\theta} \tag{12}$$

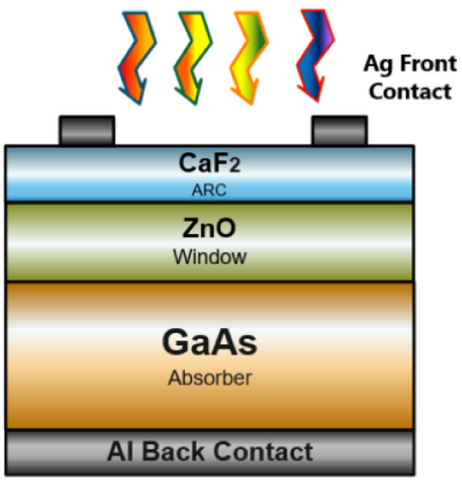

Fig. 2 Schematic diagram of proposed device

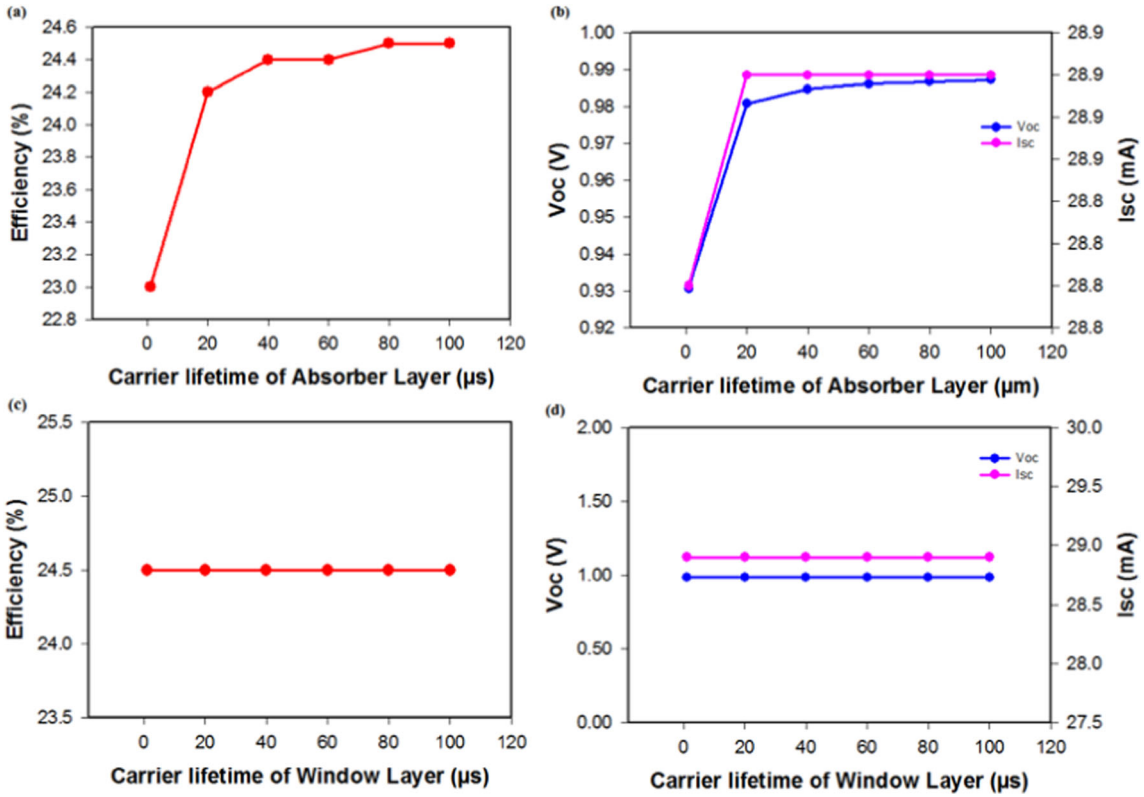

Fig. 3 Optimization of carrier lifetime (**a**) Absorber layer efficiency (**b**) I_{sc} and V_{oc} for absorber layer (**c**) Window layer efficiency (**d**) I_{sc} and V_{oc} for window layer

where, η_0 is the refractive index of air and η_2 is the refractive index of glass.

Variation in thickness of absorber and window layer from 0.5 to 4 μm and 10 to 80 μm has been investigated respectively. Parameters for GaAs and ZnO layer are selected from pervious reported articles [29, 38, 86, 91, 92]. The simulation was performed at constant intensity of 0.1 W/cm^2 and under AM 1.5 at temperature of 25 °C. The carrier lifetime was adjusted to 1–100 μs. The doping concentration of window and absorber layer has been varied from 1×10^{12} to 1×10^{18} cm^{-3}. Other parameters are listed in Table 1.

4. Result and discussion

4.1. Carrier lifetime

Carrier lifetime is critical factor to achieve high solar cell performance which plays an important role in the production of photocurrent [93]. The phenomena of lifetime and recombination are important for the collection of a high number of charge carriers. Hence, it is needed to limit carrier recombination, which may increase carrier lifetime [31]. As demonstrated in Fig. 1a, the efficiency for the absorber layer increased up to 24.5% when the carrier lifetime rises from 1 μs to 100 μs, but in case of window layer, efficiency not significantly affected by carrier lifetime. The lifetime of absorber layer against different values of V_{oc} and I_{sc} is shown in Fig. 1b. In general, for absorber layer I_{sc} and V_{oc} does not depend on carrier lifetime [31]. On the other hand, in our study V_{oc} and I_{sc} does not depend on carrier lifetime for window layer as represented in Fig. 1d. However, in case of absorber layer, the V_{oc} increased from 1 μs to 100 μs and I_{sc} shows constant trend after 20 μs, as represented in Fig. 1b.

4.2. Doping concentration

Since undesirable shunt path on absorber layer can cause a significant charge carriers concentration to damage surface of solar cell [94], concentration of doping must have to be suitable for the solar cell's optimal performance without having an adverse impact on it. The efficiency of the window and absorber layers versus doping concentration are computed in the range from 1×10^{12} to 1×10^{18} cm^{-3}. The maximum efficiency of 24.5% is noticed when the doping concentration is 1×10^{15} and 1×10^{18} cm^{-3} for absorber and window layer respectively, as shown in Fig. 2a, c. The optimum doping

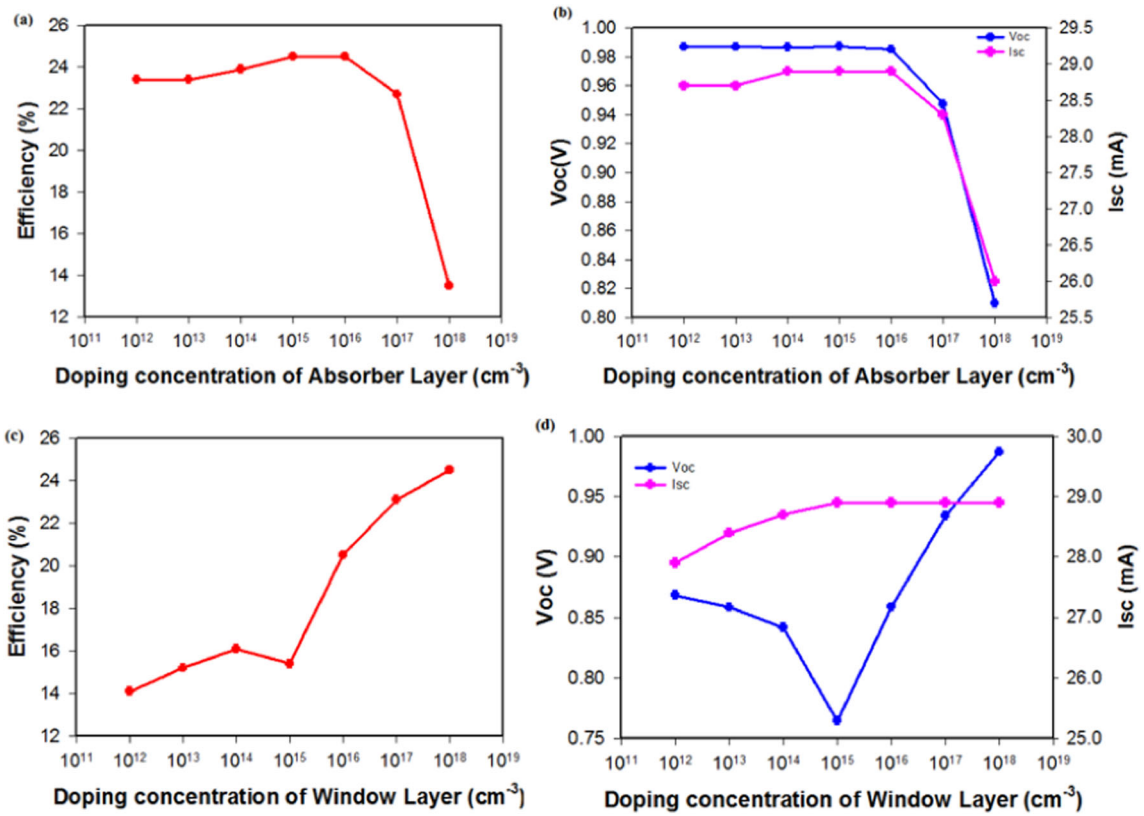

Fig. 4 Optimization of doping concentration (**a**) Absorber layer efficiency (**b**) Isc and Voc of absorber layer (**c**) Window layer efficiency (**d**) Isc and Voc of window layer

Table 2 Optimum parameters for absorber and window layers

Parameters	Absorber layer	Window layer
Thickness (μm)	70	0.5
Doping concentration (cm^{-3})	1×10^{15}	1×10^{18}
Carrier lifetime	100	100

concentration is 1×10^{15} and 1×10^{18} cm^{-3} for absorber and window layer respectively. The doping concentration in absorber and window layer provides an integral part in achieving maximum I_{sc} and V_{oc}. Voc and Isc against doping concentrations for absorber and window layer were carried in range of 1×10^{12} to 1×10^{18} cm^{-3}. The value of Isc remains constant at 28.9 mA in the range of 1×10^{14} to 1×10^{16} cm^{-3} concentration for absorber layer. When the doping concentration increased, the short circuit current rapidly decreased, as demonstrated in Fig. 2b. The reduction in V_{oc} and efficiency with increased absorber layer doping concentration may be related to changes in band structures and energy levels. High dopant content in the absorber layer may be the cause of the apparent decrease in I_{sc} value. Generally, increased doping levels in absorber layer may harm the crystal structure, as seen with GaAs, resulting in a decrease in absorption of light through the cell's surface and a drop in I_{sc} and solar cell efficiency [95]. From Fig. 3d it can be noticed that at 1×10^{18} cm^{-3} doping concentration for window layer maximum value of V_{oc} of 0.9872 V has been recorded and the value of I_{sc} is almost independent.

4.3. Thickness of window and absorber layers

When it comes to solar cells, the absorber layer's thickness is critical since it can trap more solar radiation, which leads to an improve in the number of charge carriers [96]. It has been noted that solar cells operate more efficiently when the absorber layer is thicker. In short, the absorber layer thickness not only affects the PV parameters (I_{sc} and V_{oc}) as well as the overall performance. The performance of device is influenced by the recombination process speeding up as the thickness of absorber layer increases [87, 97, 98]. The highest efficiency of 24.5% is achieved for maximum 50 μm thickness of absorber layer after 50 μm it shows a constant behavior up to 80 μm Fig. 4a. The results indicated that efficiency increased with increasing absorber layer thickness but decreased with increasing window layer thickness. The greatest efficiency was 24.5% at 0.5 μm

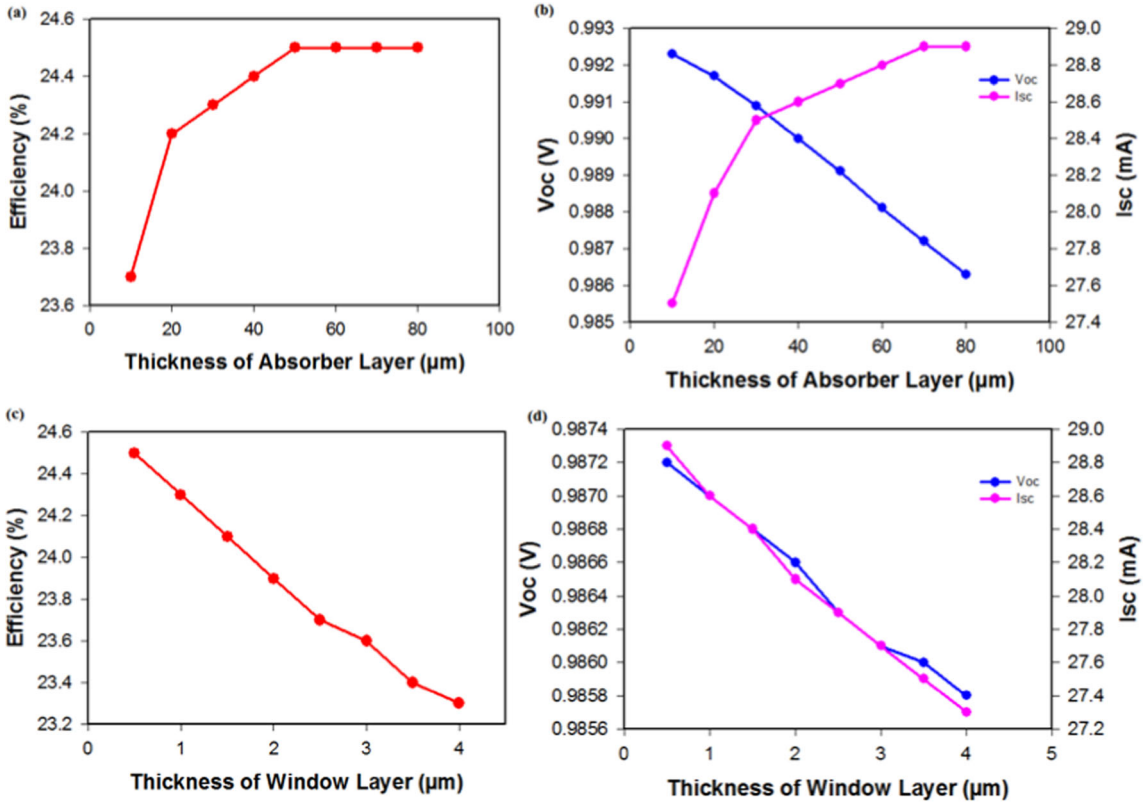

Fig. 5 Optimization of Thickness (**a**) Efficiency of absorber layer (**b**) Voc and Isc of absorber layer (**c**) Efficiency of window layer (**d**) Voc and Isc of window layer

window layer thickness but it decreased to 23.3% by further increasing the thickness to 4 μm, as shown in Fig. 4c. This section has also analyzed how window and absorber layer thickness affects V_{oc} and I_{sc}. Since I_{sc} increases and V_{oc} reduced with the increment in thickness of absorber layer because of nature of solar cell (Fig. 4b). The maximum values of I_{sc} and V_{oc} were recorded to be 28.9 mA for thickness of 70 μm and 0.9923 V for a thickness of 10 μm, respectively. On the other hand, I_{sc} and V_{oc} decreased with the increment in thickness of window layer from 0.5 to 4 μm as demonstrated in Fig. 4d. The highest values of I_{sc} and V_{oc} were observed to be 28.9 mA and 0.9872 V for a thickness of 0.5 μm. Thus, the optimum thickness for window and absorber layers is 0.5 and 70 μm respectively. Optimum parameters of absorber and window layer are shown in Table 2.

4.4. ARC layer

The ARC layer is a critical factor for the improvement of solar cell performance by decreasing reflectance, increasing conversion efficiency, Isc and absorbing photons from incident light source. In solar cells there is a high possibility of optical loss throughout the photoelectric effect, which impacts the solar cell efficiency [99]. Hence, ARC is applied to prevent reflection loss and can also enhance the photocurrent. Moreover, the impact of ARC layer is more appropriate in the range of 500–700 nm for spectrum loss [100]. Figure 5 demonstrates the refractive index of CaF_2 with respect to wavelength. The reflectance, external quantum efficiency (EQE) and I-V characteristics at different thickness along with their respective refractive index as demonstrated in Fig. 6. Minimum reflectance for refractive index n = 1.434 with 104.6 nm thickness at wavelength of 600 nm can be observed from Fig. 6, while maximum current and EQE for 1.434 refractive index with 104.6 nm thickness are presented in Fig. 6b and c. According to Fig. 6c maximum I_{sc} = 32 mA is attained at n = 1.434 with 104.6 nm thickness of layer. The current is among the simplest factor that may be improved by considerable edge. Hence it is essential to list the sources of I_{sc} deficit. The maximum R_{av}% was observed at 200 nm wavelength for n = 1.495. it can be observed that EQE is significantly increased due to reduction of reflection by applying ARC material (CaF_2). Overall EQE at n = 1.434 with 104.6 nm shows the best results.

Table 3 shows that variation in thickness with their respective wavelength modifies the reflectance R_{av} (%), I_{sc}, V_{oc}, P_{max}, and η (%). The ARC layer thickness can be adjusted because the absorption coefficient, excitation

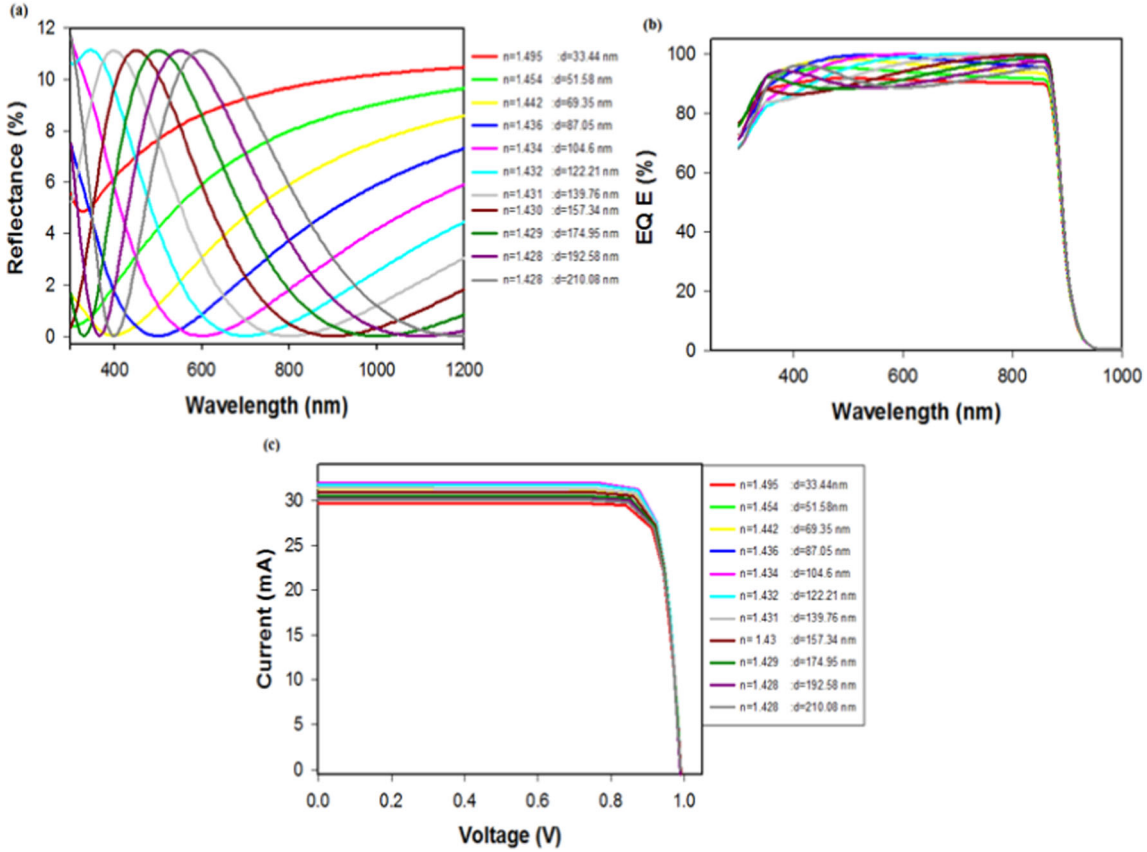

Fig. 6 Analysis with respect to their refractive index (**a**) reflectance (**b**) EQE (**c**) I-V curves for CaF_2

coefficient, and refractive index are wavelength dependent but to attain optimum absorption that cannot be adjusted easily. R_{av} (%) of CaF_2 as ARC layer at 200–1200 nm is 8.83, 6.57, 4.71, 3.69, 3.37, 3.38, 3.43, 3.46, 3.65, 4.12, and 4.82% respectively. The optimum thickness of 104.6 nm for CaF_2 ARC layer at 600 nm achieved the maximum efficiency of 27.4% with 3.37% average reflectance as shown in Table 3. From Fig. 7 it can be observed that minimum R_{av} (%) is at n = 1.434 with 104.6 nm of CaF_2 layer at 600 nm. I-V parameters are also represented in Table 3 at various refractive index according to their wavelengths in the range of 200–1200 nm. The I_{sc} values are 29.7, 30.5, 31.3, 31.8, 32, 31.8, 31.4, 30.9, 30.5, 30.3, and 30.1 mA for wavelength range of 200–1200 nm. The outcomes achieved for I_{sc} associate well with R_{av} (%) values of CaF_2 ARC layer.

Table 3 Optoelectronic properties of CaF_2 ARC layer

λ (nm)	Refractive index	Thickness (nm)	*Rav* (%)	I_{sc} (mA)	V_{oc} (V)	P_{max} (W)	FF (%)	η (%)
200	1.495	33.44	8.83	29.7	0.9879	0.0251	85.54	25.1
300	1.454	51.58	6.57	30.5	0.9886	0.0260	86.22	26.0
400	1.442	69.35	4.71	31.3	0.9893	0.0268	86.54	26.8
500	1.436	87.05	3.69	31.8	0.9898	0.0273	86.73	27.3
600	1.434	104.6	3.37	32.0	0.9899	0.0274	86.49	27.4
700	1.432	122.21	3.38	31.8	0.9897	0.0272	86.42	27.2
800	1.431	139.76	3.43	31.4	0.9894	0.0268	86.26	26.8
900	1.43	157.34	3.46	30.9	0.9890	0.0264	86.38	26.4
1000	1.429	174.95	3.65	30.5	0.9887	0.0260	86.22	26.0
1100	1.428	192.58	4.12	30.3	0.9884	0.0257	85.81	25.7
1200	1.428	210.08	4.82	30.1	0.9883	0.0255	85.72	25.5

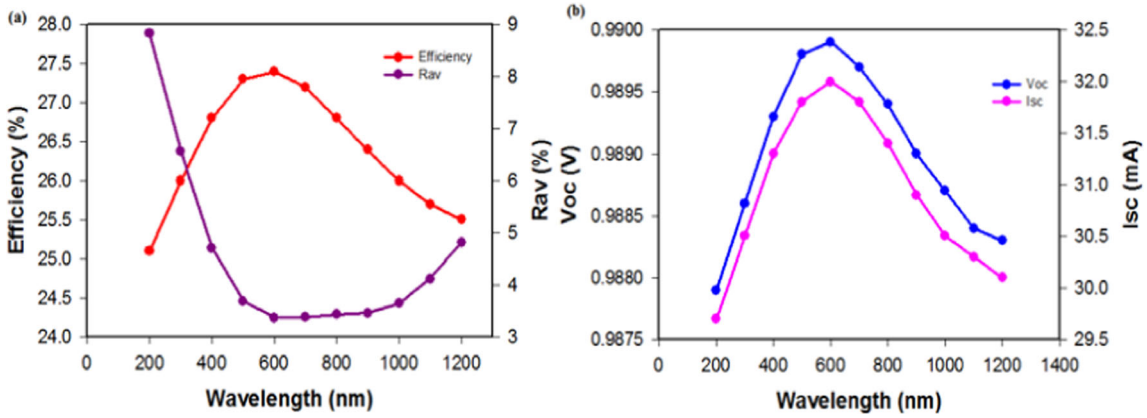

Fig. 7 Factors that influence performance of solar cell by CaF_2 ARC

Table 4 Reflectance analysis of CaF_2 ARC layer

ARC (CaF_2)	Reflectance (%) at 500 nm	Reflectance (%) at 600 nm	Reflectance (%) at 700 nm	η (%)
λ = 500 nm with d = 87.05 nm	0.023	0.851	2.317	27.3
λ = 600 nm with d = 104.6 nm	1.185	0.019	0.634	27.4
λ = 700 nm with d = 122.21 nm	4.133	0.849	0.015	27.2

From Fig. 7 efficiency trend can be observed with respect to designed wavelength from 200 to 1200 nm. The efficiency increased from 200 to 600 nm with corresponding optimal thickness and highest efficiency is attained at 600 nm, and then begins reducing from 700 to 1200 nm for CaF_2 ARC as also shown in Table 3.The maximum efficiency of 27.4% is attained with n = 1.434. The average reflectance values (R_{av}%) were calculated in the range of 300–1200 nm wavelength for CaF_2. Figure 7 depicts the trend of average reflectance. Lowest reflectance observed at 600 nm wavelength. If CaF_2 is designed for 600 nm wavelengths and then reflectance at 500, 600, and 700 nm is 1.185, 0.019, 0.634% respectively (Table 4). It can be notice that minimum reflectance is achieved with the wavelength and their respective thickness for which layer is designed. Hence for all ARC the values of reflectance drop to that wavelength with their subsequent thickness for which layer was constructed.

In this work the variation in thickness of different layers from 50 to 140 nm has been done chosen. The impact of layer thickness on V_{oc} and I_{sc} was investigated from 50 to 140 nm as indicated in Fig. 8. Among all materials, the uppermost value of I_{sc} = 32 mA and V_{oc} = 0.989 V has been noted at 100 nm of thickness of CaF_2 and MgF_2 ARC layer as demonstrated in Fig. 8b and c. Additionally, the efficiency increased as the ARC layer's thickness increased up to 100 nm before beginning to drop again at higher ARC layer thicknesses (Fig. 8 a). The optimum thickness and efficiency are 110, 90, 80, 80, 90 and 100 nm and 27.4, 26.8, 26.4, 26, 27.3 and 27.4% with MgF_2, Al_2O_3, MgO, TiN, SiO_2 and CaF_2 ARC for solar cell. The decrease in light reflection is indeed the reason for this increasing efficiency [101].

The average spectral reflectance of different ARC layers has been recorded to be 3.40, 4.99, 5.90, 6.85, 3.49, and 3.37% for MgF_2, Al_2O_3, MgO, TiN, SiO_2 and CaF_2 respectively in wavelength range of 200–1200 nm. The reflectance analysis indicated that CaF_2 as single layer demonstrated the minimum R_{av} (3.37%) as shown in Fig. 9a. The black line denotes the general representation of the solar cell for an ideal (0%) ARC material. It is sufficient to say from the reflectance curves, when reflection is reduced from surface the efficiency improved. The quantum efficiency (QE) measures how many charges are absorbed by solar cell in relation to how many photons with a particular amount of energy hit on it [102]. Figure 9b illustrates the EQE of solar cell for different ARC materials. In this study the application of ARC layers increased the EQE which could be attributed to minimized the reflection of the solar spectrum by ARC. Without any ARC material, the quantum efficiency of solar cells is around 89%, but adding an ARC layer in the 300–1200 nm wavelength range has significantly increased it as shown in Fig. 9b.The EQE of ZnO/GaAs solar cell reached its

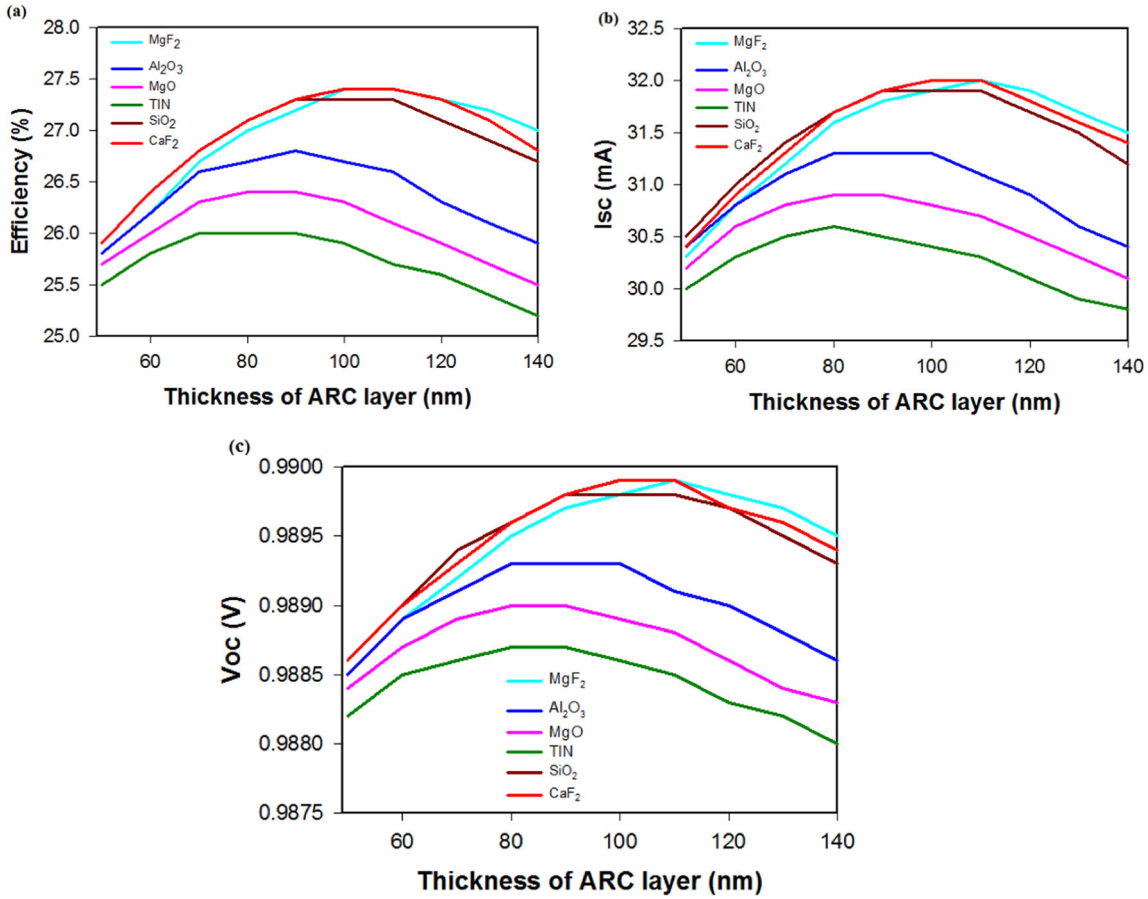

Fig. 8 Analysis of (**a**) efficiency (**b**) Isc (**c**) Voc as function of different ARC layer

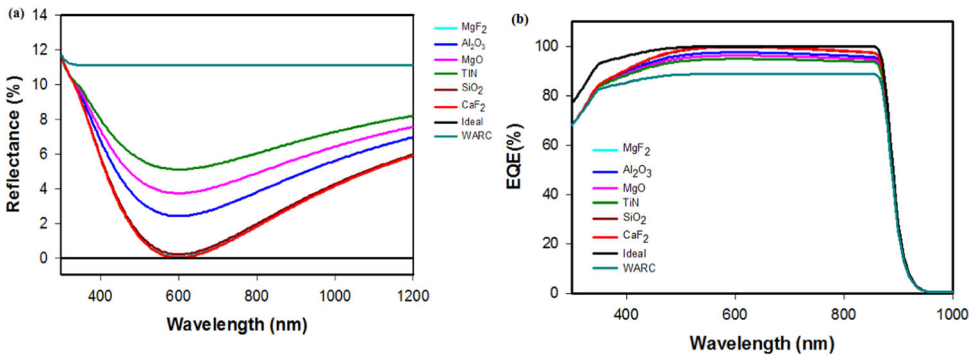

Fig. 9 Optical analysis of Different ARC layers (**a**) Reflectance (**b**) EQE

highest percentage 99.8% for CaF_2 and MgF_2 ARC layer and for ideal case its almost 99.9% as shown in Fig. 9b. The absorption of high energy photons with ARC layers is mostly accountable for poor EQE at shorter wavelength.

The cumulative photogeneration rate is determined by number of electrons produced at each location in the solar cell as a result of photon absorption [93]. The photogeneration in solar cell is investigated with ARC materials such as MgF_2, Al_2O_3, MgO, TiN, SiO_2, CaF_2 and also without any ARC material. It was observed that photogeneration rate initiates from zero and progressively increased with the increasing distance from front in the solar cell (Fig. 10b). The photogeneration rate 201 $\times$ 10^{15}/sec with CaF_2 and MgF_2 ARC layer is greater than other materials, whereas without any layer, the low generation rate (181 $\times$ 10^{15}/sec) was recorded as shown in Fig. 10b. Ideal case shows the 204 $\times$ 10^{15}/sec cumulative photogeneration rate. The I-V curve of ZnO/GaAs solar cell with different ARC materials and without any layer are shown in Fig. 10a. The results demonstrated that highest I_{sc} (32 mA) and V_{oc} (0.989 V) was obtained using CaF_2 and MgF_2 ARC layer (Fig. 10).

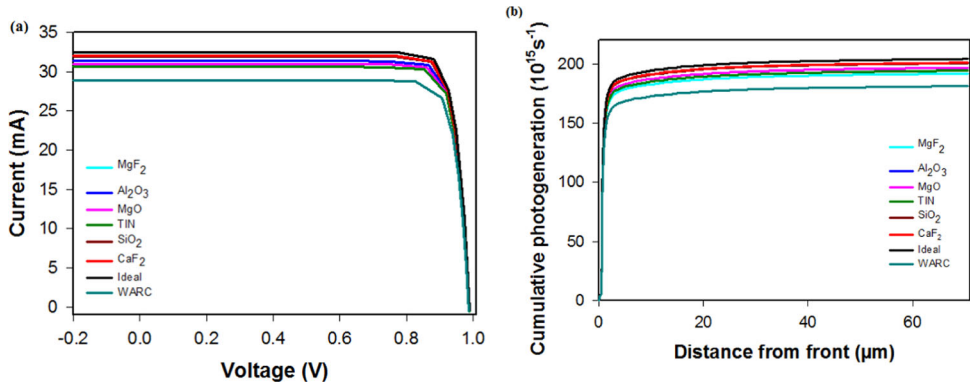

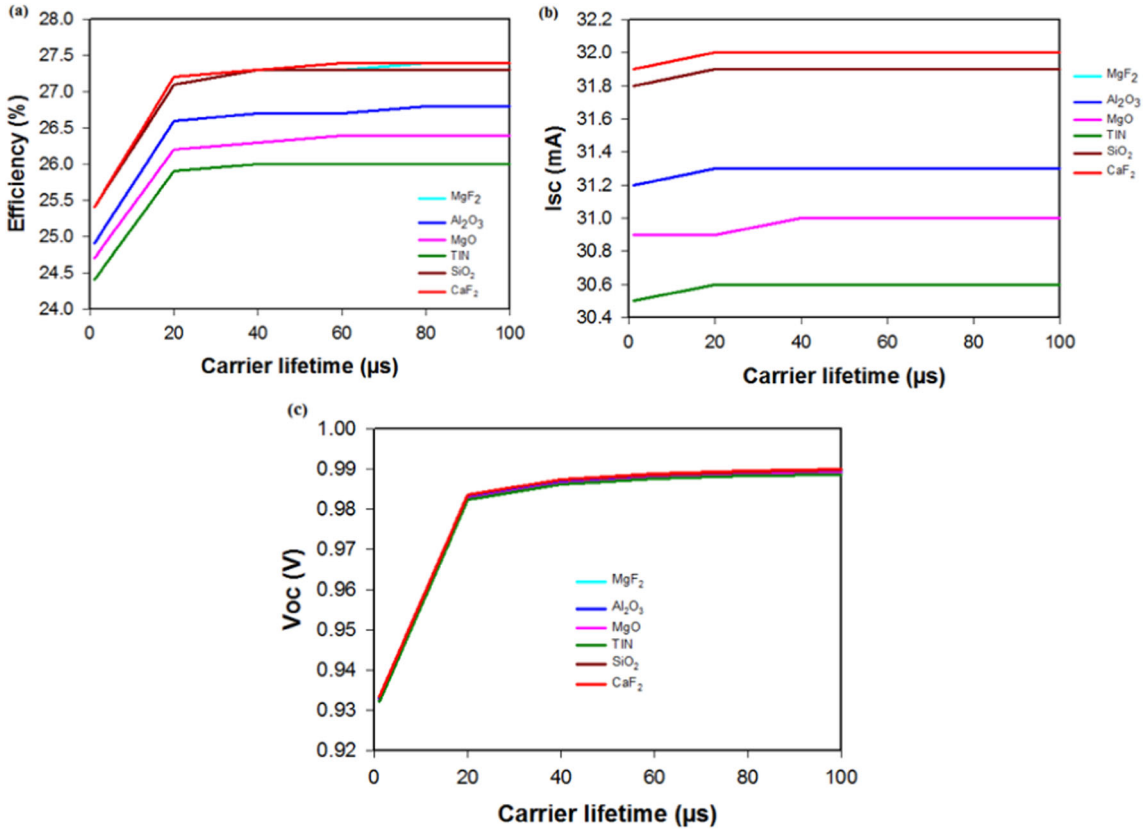

Fig. 10 Analysis of different ARC layer (**a**) IV-curves (**b**) cumulative photogeneration rate

Fig. 11 Analysis of Carrier lifetime versus **a** Efficiency **b** Isc **c** Voc

Since carrier lifetime is crucial for achieving outstanding performance in solar cells and hence, as the carrier lifetime of a solar cell grows, so does its efficiency and I_{sc} [93]. The I-V is the ultimate parameter which confirmed the fruitful application of CaF_2 and MgF_2 as ARC layer in GaAs based solar cell. When we adjusted the carrier lifetime in the range 1–100 μs, the efficiency increased in each ARC layer (Fig. 11a). Among different ARC materials, the results showed that CaF_2 and MgF_2 ARC layer has maximum efficiency along with maximum V_{oc} and I_{sc} values (Fig. 11b).Thus from all analysis we concluded that MgF_2 and CaF2 shows best results as compared to other ARC materials for ZnO/GaAs solar cell as shown in Table 5. If we consider a stability factor that is also a most important parameter for the choice of ARC layer, then we can say that CaF_2 is appropriate choice of material for ARC layer. Table 6 represents the comparative analysis of GaAs Based solar cell.

5. Conclusions

A numerical investigation has been carried out to analyze the effect of doping concentration, carrier lifetime and

Table 5 Comparative analysis of different ARC layers with CaF_2 ARC layer

ARC Materials	Refractive index	Thickness (nm)	R_{av} (%)	*Isc* (mA)	V_{oc} (V)	P_{max} (W)	*FF*	η (%)
MgF_2	1.38	108.7	3.40	32.0	0.9899	0.0274	86.49	27.4
Al_2O_3	1.654	90.7	4.99	31.3	0.9893	0.0268	86.54	26.8
MgO	1.72	87.2	5.90	31	0.989	0.0264	86.11	26.4
TiN	1.78	84.3	6.85	30.6	0.9887	0.0260	85.93	26.0
SiO_2	1.48	101.4	3.49	31.9	0.9898	0.0273	86.46	27.3
CaF_2	1.434	104.6	3.37	32.0	0.9899	0.0274	86.49	27.4
WARC	–	–	11.12	28.9	0.9872	0.0245	85.87	24.5
Ideal	–	–	0	32.5	0.9903	0.0278	86.37	27.8

Table 6 Comparative analysis with reported results based on GaAs solar cells

Types of solar cell	Isc (A)	Voc (V)	FF (%)	η (%)	Reference
GaAs homojunction	2.70	0.98	83.35	22.08	[91]
With graphene layer	8.191	0.389	0.548	2.218	[21]
Homojunction	2.288	1.08	84	21	[92]
InAs/GaAs	2.253	0.983	83.9	14.1	[93]
Without ARC CdS/GaAs	2.65	0.882	89.40	20.88	[3]
With Al_2O_3 ARC layer CdS/GaAs	3.11	0.884	89.44	24.60	[3]
CaF_2 Anti-Reflection Coatimg	–	–	–	19.35	[103]
CaF_2/ITO	0.04083	–	81.06	21	[104]
With CaF_2 ARC	0.032	0.9899	86.49	27.4	This work
Without ARC	0.0289	0.9872	85.87	24.5	This work
ZnO/GaAS (ideal case)	0.0325	0.9903	86.37	27.8	This work

ARC layer thickness on the performance of solar cell. The optimum values of different parameters such as doping concentration, thickness of layers and carrier lifetime are well simulated to design highly efficient ZnO/GaAs solar cell. The outstanding efficiency of 27.8% has been attained for ideal case and 27.4% for MgF_2 and CaF_2. Without any ARC layer the device shows 24.5% PCE at 0.5 μm thickness of window layer and 70 μm of absorber layer width. The optimal carrier lifetime for absorber, window, and Arc layer is 100 μs. The study revealed that CaF_2 and MgF_2 are the potential candidate for high efficiency as compared to other ARC materials. Results revealed that MgF_2 and CaF_2 show almost same results as ARC layer but when it comes to stability CaF_2 is more appropriate material as ARC layer for ZnO/GaAS solar cell.

Acknowledgements This work was supported by the Higher Education Commission (HEC) of Pakistan [Grant No: 8615/Punjab/NRPU/R&D/HEC/2017] to Dr. Khuram Ali.

Declarations

Conflict of interest The authors declare that they have no known competing financial interests or personal relationships that could have appeared to influence the work reported in this paper.

References

[1] Taylor P International Energy Agency. (2010)
[2] N S Lewis, G Crabtree, A Nozik, M Wasielewski, P Alivisatos, H Kung et al. Basic research needs for solar energy utilization. Report of the basic energy sciences workshop on solar energy utilization, 18–21, (2005). DOESC (USDOE Office of Science (SC))
[3] D K Shah, K Devendra, D Parajuli, M S Akhtar, C Y Kim and O-B Yang *Solar energy* **234** 330 (2022)
[4] T B McKee *Water* **26** 1 (1993)
[5] D K Shah *Chemical physics letters* **754** 137756 (2020)
[6] G D Barber et al *The journal of physical chemistry letters* **2** 581 (2011)
[7] J Fang, H Wu, T Liu, Z Zheng, J Lei, Q Liu et al *Applied Energy* **279** 115778 (2020)
[8] H Li, Y Hu, H Wang, Q Tao, Y Zhu and Y Yang *Solar RRL* **5** 3 2000524 (2021)
[9] M Alaaeddin, S Sapuan, M Zuhri, E Zainudin and F M Al-Oqla *Renewable and Sustainable Energy Reviews* **102** 318 (2019)

[10] Q Ni *Journal of Quantitative Spectroscopy and Radiative Transfer* **268** 107625 (2021)
[11] K Islam, A Nayfeh Simulation of a-Si/c-GaAs/c-Si heterojunction solar cells. In: 2012 Sixth UKSim/AMSS European Symposium on Computer Modeling and Simulation. (2012). IEEE
[12] B M Kayes et al. 27.6% conversion efficiency, a new record for single-junction solar cells under 1 sun illumination. In: 2011 37th IEEE Photovoltaic Specialists Conference. (2011). IEEE
[13] S B Khan, S Irfan, Z Zhuanghao and S L Lee *Materials* **12** 1483 (2019)
[14] M-C Tseng *IEEE Electron Device Letters* **30** 940 (2009)
[15] Z Dai, S Chegwidden, L Rumaner and F Ohuchi *Journal of Applied Physics* **85** 2603 (1999)
[16] K Devendra *Am. J. Eng. Res* **9** 218 (2020)
[17] G Jarosz *Materials Science in Semiconductor Processing* **107** 104812 (2020)
[18] L M Herz *ACS Energy Letters* **2** 1539 (2017)
[19] M Sotoodeh *Journal of Applied Physics* **87** 2890 (2000)
[20] A D Khan, A D Khan *Applied Physics A* **124**(12) 851 (2018)
[21] Y Kuang, Y Liu, Y Ma, J Xu, X Yang, X Hong et al *Advances in Condensed Matter Physics* (2015). https://doi.org/10.1155/2015/326384
[22] E T Mohamed, A O Maka, M Mehmood, A M Direedar and N Amin *Sustainable Energy Technologies and Assessments* **44** 101067 (2021)
[23] N Gruginskie et al *Solar Energy Materials and Solar Cells* **223** 110971 (2021)
[24] V Ranjan, C S Solanki, R Lal. Minority carrier lifetime, measurement of solar cell. In: 2008 2nd National Workshop on Advanced Optoelectronic Materials and Devices. (2008). IEEE
[25] Z Ali, K Ali, B Hussain, S Maqsood and I Iqbal *Optical Materials* **128** 112358 (2022)
[26] D K Shah, S Y Han, S M Akhtar, O Yang and C Y Kim *Nanoscience and Nanotechnology Letters* **11** 159 (2019)
[27] V A Coleman, C Jagadish, Basic properties and applications of ZnO, in Zinc oxide bulk, thin films and nanostructures. 2006, Elsevier. p. 1-20
[28] Y Liu, Y Li, Y Wu, G Yang, L Mazzarella, P Procel-Moya et al *Materials Science and Engineering: R: Reports* **142** 100579 (2020)
[29] H Naim, D K Shah, A Bouadi, M R Siddiqui, M S Akhtar and C Y Kim *Journal of Electronic Materials* **51** 586 (2022)
[30] B Hussain, M Y A Raja, N Lu, I Ferguson. Applications and synthesis of zinc oxide: an emerging wide bandgap material. In: 2013 High Capacity Optical Networks and Emerging/Enabling Technologies. (2013). IEEE
[31] D K Shah, K Devendra, M Muddassir, M S Akhtar, C Y Kim and O-B Yang *Solar energy* **216** 259 (2021)
[32] D K Shah, D KC, M S Akhtar, C Y Kim and O-B Yang *Applied Sciences* **10** 6062 (2020)
[33] D K Shah, J Choi, D KC, M S Akhtar, C Y Kim and O-B Yang *Journal of Materials Science: Materials in Electronics* **32** 2784 (2021)
[34] K Islam, A Alnuaimi, H Ally, A Nayfeh. ITO, Si3N4 and ZnO: Al-Simulation of Different Anti-reflection Coatings (ARC) for Thin Film a-Si: H Solar Cells. In: 2013 European Modelling Symposium. (2013). IEEE
[35] D K Shah *Optical Materials* **121** 111500 (2021)
[36] D Hocine, M Belkaid, M Pasquinelli, L Escoubas, J Simon, G Rivière et al *Materials Science in Semiconductor Processing* **16** 113 (2013)
[37] D K Shah et al *Materials Science in Semiconductor Processing* **147** 106695 (2022)
[38] L Dobrzański, M Szindler, A Drygała and M Szindler *Open Physics* **12** 666 (2014)
[39] R Sharma, G Amit, V Ajit. (2017).
[40] A Sultanov *Materials Today: Proceedings* **49** 2511 (2022)
[41] Periyasamy B D D S.
[42] P Ilenikhena *Physics* **11** 415 (2007)
[43] N Venugopal, V Gerasimov, A Ershov, S Karpov and S Polyutov *Optical Materials* **72** 397 (2017)
[44] M Chinnasamy, R Rathanasamy, S Sivaraj, G Velu Kaliyannan, M S Anbupalani and S K Jaganathan *Journal of Electronic Materials* **51** 2833 (2022)
[45] Robin R Phillips, Vic Haynes, David A Naylor and Peter Ade *Applied Optics* **47** 870 (2008). https://doi.org/10.1364/AO.47.000870
[46] Mushtak Abdulmohsen Jabbar and Tariq J Alwan *Iraqi Journal of Science* (2020). https://doi.org/10.24996/ijs.2020.61.11.13
[47] N M Saeed and A Suhail *Iraqi journal of science* **53** 88 (2012)
[48] Faiazul Haque, Kazi Sajedur Rahman, Mohammad Aminul Islam, Yulisa Yusoff, Naveed Aziz Khan, Ammar Ahmed Nasser and Nowshad Amin *Optical and Quantum Electronics* (2019). https://doi.org/10.1007/s11082-019-1994-6
[49] Feng Zhan, Ji-Fang He, Xiang-Jun Shang, Mi-Feng Li, Hai-Qiao Ni, Xu Ying-Qiang and Zhi-Chuan Niu *Chinese Physics B* **21** 037802 (2012). https://doi.org/10.1088/1674-1056/21/3/037802
[50] M Fedawy, S M Ali and T Abdolkader *Journal of Advanced Research in Materials Science* **42** 1 (2018)
[51] Y-Y Quan and L-Z Zhang *Solar Energy Materials and Solar Cells* **160** 382 (2017)
[52] Xiaoyu Sun, Lei Li, Xu Xiaozhuang, Guanyu Song, Tu Jielei, Pingyuan Yan, Weinan Zhang and Hu Kai *Optik* **212** 164704 (2020). https://doi.org/10.1016/j.ijleo.2020.164704
[53] M A Contreras, B Egaas, K Ramanathan, J Hiltner, A Swartzlander, F Hasoon et al *Progress in Photovoltaics: Research and applications* **7** 311 (1999)
[54] A Alemu, A Freundlich, N Badi, C Boney and A Bensaoula *Solar Energy Materials and Solar Cells* **94** 921 (2010)
[55] A S Sarkın *Solar energy* **199** 63 (2020)
[56] Ke Ding, Xiujuan Zhang, Ling Ning, Zhibin Shao, Peng Xiao, Anita Ho-Baillie, Xiaohong Zhang and Jiansheng Jie *Nano Energy* **46** 257 (2018). https://doi.org/10.1016/j.nanoen.2018.02.005
[57] Fu Wei Li, Ting Shu Lv, Xinyu Tan, Lihua Jiang, Ting Xiao and Peng Xiang *Materials Letters* **243** 108 (2019). https://doi.org/10.1016/j.matlet.2019.01.158
[58] N Rezaei, O Isabella, Z Vroon and M Zeman *Solar energy* **177** 59 (2019)
[59] N H Kumar, D Ravinder, T A Babu, N Venkatesh, S Swathi and N K Prasad *Journal of the Indian Chemical Society* **99** 100362 (2022)
[60] N H Kumar, A Edukondalu and D Ravinder *Journal of the Australian Ceramic Society* **11** 1 (2023)
[61] J Doualan, P Camy, R Moncorgé, E Daran, M Couchaud and B Ferrand *Journal of Fluorine Chemistry* **128** 459 (2007)
[62] A De Bonis, A Santagata, A Galasso, M Sansone and R Teghil *Applied surface science* **302** 145 (2014)
[63] H Wang, R Liu, K Chen, X Shi and Z Xu *Thin Solid Films* **519** 6438 (2011)
[64] J Mashaiekhy, Z Shafieizadeh, H Nahidi and I Hadi *Optik* **124** 3957 (2013)
[65] I Snetkov *Optical Materials* **69** 291 (2017)
[66] L Yan, F Qin Dong, S Zhao, H Yan, H Lv and X Yuan *Materials Letters* **129** 158 (2014)
[67] R Yadav, A Mittal, S Dwivedi and A Pandey *Surface and interface analysis* **45** 1775 (2013)
[68] J Sun, Y Zhang, Y Zheng, Z Xu and R Liu *Thin Solid Films* **562** 478 (2014)
[69] Xixi Liu, Hu Xiaoyun, Hui Miao, Guowei Zhang, Mu Jianglong, Tongxin Han and Dekai Zhang *Solar Energy* **134** 45 (2016). https://doi.org/10.1016/j.solener.2016.04.047

[70] V Ludhiya *Inorganic Chemistry Communications* **150** 110558 (2023)
[71] E Sumalatha *Inorganic Chemistry Communications* **146** 110200 (2022)
[72] M-C Liu, C-C Lee, M Kaneko, K Nakahira and Y Takano *Applied Optics* **45** 1368 (2006)
[73] R Thielsch, M Pommies, J Heber, N Kaiser, J Ullmann. Structural and mechanical properties of evaporated pure and mixed MgF2-BaF2 thin films. In: Advances in Optical Interference Coatings. (1999). SPIE
[74] N Emre Çetin, Şadan Korkmaz, Saliha Elmas, Naci Ekem, M Suat Pat, Zafer Balbağ, Enver Tarhan, Sinan Temel and Murat Özmumcu *Materials Letters* **91** 175 (2013). https://doi.org/10.1016/j.matlet.2012.07.086
[75] Chao Wen and Mario Lanza *Applied Physics Reviews* (2021). https://doi.org/10.1063/5.0036987
[76] A Rehmer *Journal of Materials Chemistry C* **3** 1716 (2015)
[77] C A Lucas and D Loretto *Applied Physics Letters* **60** 2071 (1992). https://doi.org/10.1063/1.107092
[78] S Sinharoy *Thin Solid Films* **187** 231 (1990)
[79] Yijia Huang, Pu Mingbo, Zeyu Zhao, Xiong Li, Xiaoliang Ma and Xiangang Luo *Optics Communications* **407** 204 (2018). https://doi.org/10.1016/j.optcom.2017.09.036
[80] R Reeves *Journal of Luminescence* **129** 1673 (2009)
[81] R K Jain, J Kaur, A Khanna and A K Chawla *Journal of Materials Science: Materials in Electronics* **31** 14241 (2020)
[82] Masahiko Daimon and Akira Masumura *Applied Optics* **41** 5275 (2002). https://doi.org/10.1364/AO.41.005275
[83] K C Devendra, Deb Kumar Shah, M Shaheer Akhtar, Mira Park, Chong Yeal Kim and O-B Yang, *Molecules* **26** 3275 (2021). https://doi.org/10.3390/molecules26113275
[84] M Labed, N Sengouga, A Meftah, A Meftah and Y S Rim *Optical Materials* **120** 111453 (2021)
[85] K Dasgupta, A Mondal, S Ray, U Gangopadhyay, Silicon: p. 1, (2021)
[86] B Hussain *Solar Energy Materials and Solar Cells* **139** 95 (2015)
[87] J Bernede *Journal of the Chilean Chemical Society* **53** 1549 (2008)
[88] C F Kamdem, A T Ngoupo, F K Konan, H J T Nkuissi, B Hartiti and J-M Ndjaka *Indian Journal of Science and Technology* **12** 37 (2019)
[89] M A N D O N G Al-montazer and Ü Z Ü M Abdullah *Sakarya University Journal of Science* **23** 1190 (2019). https://doi.org/10.16984/saufenbilder.557490
[90] Gokul Sidarth Thirunavukkarasu, Mehdi Seyedmahmoudian, Jaideep Chandran, Alex Stojcevski, Maruthamuthu Subramanian, S Raj Marnadu, Mohd Alfaify and Shkir *Energies* **14** 4986 (2021). https://doi.org/10.3390/en14164986
[91] A J Thosar *Journal of Science and Technology* **7** 637 (2014)
[92] Jaker Hossain *Journal of Physics Communications* **5** 085008 (2021). https://doi.org/10.1088/2399-6528/ac1bc0
[93] M Basher *Optik* **176** 93 (2019)
[94] K Devendra *Materials Today: Proceedings* **49** 2580 (2022)
[95] Samer H Zyoud, Ahed H Zyoud, Naser M Ahmed, Anupama R Prasad, Sohaib Naseem Khan, Atef F. I Abdelkader and Moyad Shahwan *Crystals* **11** 1468 (2021). https://doi.org/10.3390/cryst11121468
[96] S Asahi, H Teranishi, K Kusaki, T Kaizu and T Kita *Nature communications* **8** 1 (2017)
[97] Neha Thakur and Rajesh Mehra *Journal of Nanoelectronics and Optoelectronics* **14** 217 (2019). https://doi.org/10.1166/jno.2019.2476
[98] H Jee, J Song, D Moon, J Lee and C Jeong *Journal of Nanoscience and Nanotechnology* **20** 7096 (2020)
[99] L Kosyachenko *Materials for Renewable and Sustainable Energy* **2** 1 (2013)
[100] Natarajan Shanmugam, Rishi Pugazhendhi, Rajvikram Madurai Elavarasan, Pitchandi Kasiviswanathan and Narottam Das *Energies* **13** 2631 (2020). https://doi.org/10.3390/en13102631
[101] B Kumaragurubaran, S Anandhi. Reduction of reflection losses in solar cell using anti reflective coating. In: 2014 International Conference on Computation of Power, Energy, Information and Communication (ICCPEIC). (2014). IEEE
[102] Markvart T and L Castañer, Principles of solar cell operation, In: McEvoy's Handbook of Photovoltaics, Elsevier. p. 3-28, (2018)
[103] C Ma, L Wang, X Fan and J Liu *Applied Surface Science* **560** 149924 (2021)
[104] M A Zahid, M Q Khokhar, Y Kim and J Yi *Crystal Research and Technology* **57** 2100233 (2022)